

Feedback control of spiral waves in a cellular automata model of excitable media

Hiroko Yoneshima, Keiji Konishi[†], and Hideki Kokame

Osaka Prefecture University
 1-1 Gakuen-cho, Naka-ku, Sakai, Osaka 599-8531 JAPAN

[†] Email: konishi@eis.osakafu-u.ac.jp

Abstract—A serious cardiac arrhythmia is well known as a main cause of cardiac sudden death. The arrhythmia is considered to be induced by spiral waves and spatio-temporal chaos in the cardiac muscle. The muscle has the characteristic feature of excitable media. This paper proposes a feedback control method for eliminating spiral waves in a cellular automata model of excitable media. The method can eliminate spiral waves by a low-amplitude pulse train. Its control performance is investigated by numerical simulations.

1. Introduction

Sudden cardiac death, which results from an abrupt loss of heart function, has been widely known and considered as a major health problem. The leading cause of death is the abnormal rhythm (e.g., fibrillation) occurred in a heart. In order to eliminate the arrhythmia and restore the regular rhythm, a high-voltage electric shock is applied to the patients' chest. This shock often imposes physical and mental strain on the patients. Hence, a therapy based on a low-voltage electric shock is now expected to be developed for practical use [1, 2].

It is well known that the abnormal rhythm would be caused by the electrical spiral waves and spatio-temporal chaotic waves occurred in the cardiac tissue [1]. The tissue can be treated as excitable media, since an electric signal propagate through the tissue without damping. The abnormal rhythm on the cardiac tissue can be essentially reduced to spatio-temporal behavior in excitable media. Such behavior is easily demonstrated in simple mathematical models.

For the above reasons, many researchers have proposed the various methods for eliminating spatio-temporal behavior in simple mathematical models of excitable media [1]. Most of methods for eliminating spatio-temporal behavior employ the non-feedback control except for a few papers [3, 4]. The non-feedback control methods are classified into two types: global and non-global. The global methods apply an input signal to every region of the medium [5]~[11], and would correspond to a high-voltage electric shock applied to the patients' chest (i.e., conventional ex-

ternal defibrillators). On the contrary, the non-global methods inject an input signal into parts of media, such as boundary [12]~[15], points [16]~[20], and grid [1, 21, 22]. The non-global methods might be realized by implantable cardioverter-defibrillators.

For development of conventional external defibrillators, it would be crucial to consider the problem how to determine the appropriate timing of the electric shock. Thus, it is important to consider the following simple and practical situation: (S1) a series of impulsive input signals can act on the whole medium; (S2) an average level of excitement overall medium can be monitored. The situation might be implemented by a pair of electrodes for applying the electronic shock and a sensor for picking up the average level of excitation.

The present paper proposes a *feedback* control method, which is suitable for the above situation. This method can be considered as a global method with feedback mechanism. The control performance is investigated by numerical simulations.

2. Cellular automata (CA) model

It is well known that the excitable media can be described by the simple mathematical models: partial differential equations, coupled map lattices, and cellular automata (CA). The present paper focuses on a popular CA model of excitable media [23]¹. This model is governed by

$$\begin{cases} x_{t+1}(i, j) = F[x_t(i, j), y_t(i, j), u_t] \\ y_{t+1}(i, j) = \\ G[F[x_t(i, j), y_t(i, j), u_t], y_t(i, j), \Omega_t(i, j)] \end{cases}, \quad (1)$$

where $y_t(i, j) \in \{0, 1\}$ and $x_t(i, j) \in \{0, 1, \dots, \bar{X}\}$ are an *excitation* variable and a *recovery* variable at time step $t \in \mathbb{N}$ respectively. The integers, $i, j \in \{1, 2, \dots, N\}$, represent the cell position; the total number of cells is N^2 . The input signal $u_t \in \mathbb{N}$, which

¹The CA model is convenient to simulate complex phenomenon on computers, since its time and space are discrete. Even as it cannot describe the details of real hearts, the present paper has employed it in order to grasp the dynamics of our control systems. We have plant to extend our results obtained in the present paper to more realistic heart models.

This work was supported by KAKENHI(20560425).

does not depend on the position (i, j) , acts on the whole medium ². This corresponds to situation (S1). The nonlinear maps F, G are given by

$$F[x, y, u] := \begin{cases} \min \{x + g_u + u, \bar{X}\} & \text{if } y = 1 \\ \max \{x - g_d + u, 0\} & \text{if } y = 0 \end{cases},$$

$$G[x, y, \Omega] :=$$

$$\begin{cases} 1 & \text{if } y = 0 \text{ and } 0 \leq x < X_e \text{ and } f_e(x) < \Omega \\ 0 & \text{if } y = 1 \text{ and } X_r < x \leq \bar{X} \\ & \text{and } (f_r(x) < (2r + 1)^2 - \Omega \text{ or } x = \bar{X}) \\ y & \text{otherwise} \end{cases}.$$

The thresholds $f_e(x)$ and $f_r(x)$ are

$$f_e(x) := k_e^0 + \{r(2r + 1) - k_e^0\} \frac{x}{X_e},$$

$$f_r(x) := k_r^0 + \{r(2r + 1) - k_r^0\} \frac{x - \bar{X}}{X_r - \bar{X}}.$$

$k_e^0, k_r^0, X_e, X_r, g_u, g_d \in \mathbb{N}$ are the parameters. $r \in \mathbb{N}$ represents the radius of an extended Moore neighborhood. The neighborhood of cell (i, j) is described by $N_{i,j}^r := \{(k, l) : |k - i| \leq r \text{ and } |l - j| \leq r\}$. $\Omega_t(i, j)$ is the number of excited cells neighborhood of cell (i, j) :

$$\Omega_t(i, j) := \sum_{(k,l) \in N_{i,j}^r} y_t(k, l).$$

In general, excitable media have a stable resting state (i.e., $y_t(i, j) = x_t(i, j) = 0, \forall i, j \in \{1, \dots, N\}$ for CA model (1)). Hence, for the initial conditions around the resting state, the system without control ($u_t \equiv 0$) eventually converges on the resting state: $\lim_{t \rightarrow \infty} y_t(i, j) = x_t(i, j) = 0$. On the contrary, for the initial conditions far from the resting state (e.g., a half line of excited cells buffered on one side by refractory cells), the system exhibits spatio-temporal behavior, such as stable spiral waves and spatiotemporal chaos.

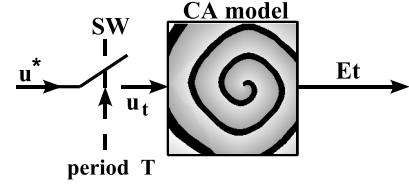
3. Feedback control

Now we assume that the total number of excited cells,

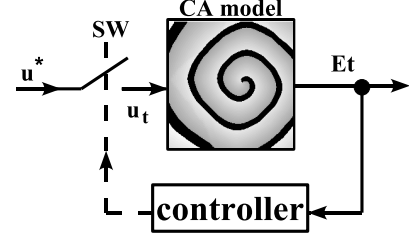
$$E_t = \sum_{i,j=1}^N y_t(i, j),$$

can be measured as an output signal. This corresponds to situation (S2). The present paper deals

²It can be considered that there are the three types of the signal injection: u_t is applied to x_t [5, 18], y_t [4, 6, 7, 9, 15, 16, 17, 19], or both of them. Since the injection to x_t allows us to grasp its effect to the media theoretically [5], the present paper purposely applies u_t to x_t .



(a) Non-feedback control



(b) Feedback control

Figure 1: Block diagrams of control systems.

with CA model (1) as a single-input ($u_t \in \mathbb{N}$) single-output ($E_t \in \mathbb{N}$) system. It should be noted that these input-output signals do not depend on the position of medium.

The main purpose of this paper is to propose the feedback controller which eliminates the spiral waves (i.e., a transition from spatio-temporal behavior to the stable resting state) by a low-amplitude input signal. Figures 1 (a) and 1 (b) illustrate the block diagrams of control systems. The proposed feedback control system is illustrated in Fig. 1 (b). A non-feedback control system shown in Fig. 1 (a) is also considered to show effectiveness of the feedback mechanism.

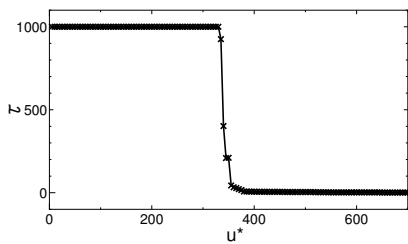
In the non-feedback control system, the switch SW is turned on at $T \in \mathbb{N}$ time step intervals. A constant value $u^* \in \mathbb{N}$ is applied as follows:

$$u_t = \begin{cases} u^* & \text{if } t \equiv 0 \pmod{T} \\ 0 & \text{otherwise} \end{cases}. \quad (2)$$

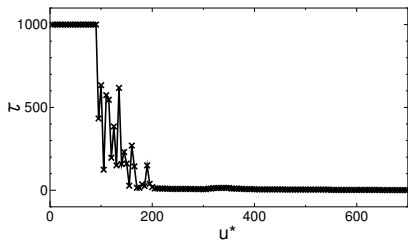
The input signal u_t is a pulse train with interval T and amplitude u^* . In contrast, the feedback controller turns on SW only when the past output signal E_{t-1} is at a local minimum: a constant value u^* is applied to all the cells in accordance with

$$u_t = \begin{cases} u^* & \text{if } E_{t-2} - E_{t-1} \geq 0 \text{ and } E_t - E_{t-1} > 0 \\ 0 & \text{otherwise} \end{cases}. \quad (3)$$

The input signal u_t is also a pulse train with amplitude u^* , but its interval depends on the past output signals.



(a) Non-feedback control



(b) Feedback control

Figure 2: Extinction time τ vs. amplitude u^* .

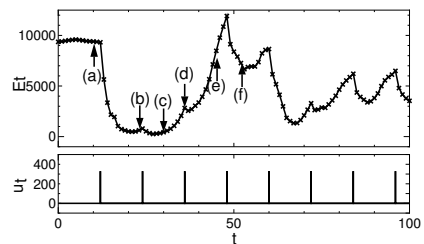
4. Numerical simulations

This section investigates the control system performances on numerical simulations. Throughout this paper, the parameter values are fixed at $r = 3$, $k_e^0 = 0$, $k_r^0 = 5$, $X_e = 850$, $X_r = 900$, $\bar{X} = 1000$, $g_u = 200$, $g_d = 50$, and $N = 200$ [23]. No-flux boundary conditions are used in all simulations. For the parameter values and the boundary conditions, CA model (1) exhibits a stable spiral wave, where E_t is a stable period-17 cycle.

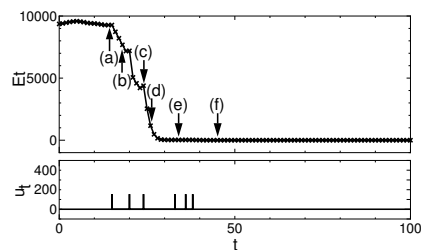
The extinction time of spiral waves, denoted by $\tau \in \mathbb{N}$, is examined both for the non-feedback and feedback control systems. This time is the elapsed time until there are no excited cells in the medium. Figure 2 shows the relation between the extinction time τ and the amplitude u^* ³. Remark that, if there are excited cells for $t > 1000$, the extinction time is set to $t = 1000$. For the non-feedback control, control law (2) with $T = 12$ and amplitude less than $u^* = 330$ cannot eliminate the spiral wave⁴. Contrastively, feedback controller (3) with amplitude $u^* = 95$ eliminates it. The time-series data of E_t and u_t for the non-feedback and feedback control systems are shown in

³Since, for the non-feedback control system, the value of τ depends on the starting time of control, the average value of τ for 17 different starting times is plotted.

⁴From our numerical simulations, we have confirmed that $T = 12$ is an optimal interval among $T=11 \sim 20$ for the elimination.



(a) Non-feedback control



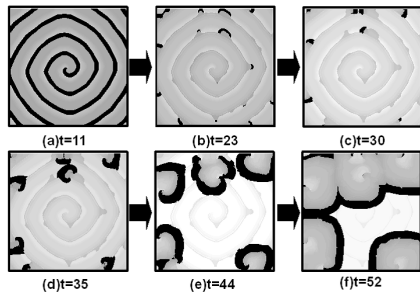
(b) Feedback control

Figure 3: Time series data of E_t , u_t .

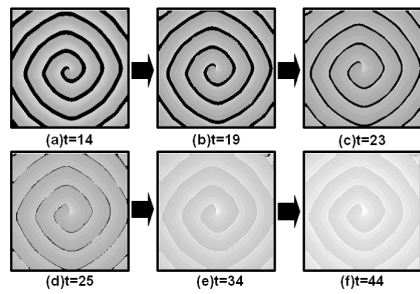
Figs. 3 (a) and 3 (b) respectively. In spite of high-amplitude signal ($u^* = 330$), E_t of the non-feedback control system fails to be zero. On the other hand, the input signal with $u^* = 155$ allows E_t monotonically to decrease with time; it eventually becomes zero. From these results, it can be seen that the proposed feedback controller effectively eliminates it compared with the non-feedback method.

Figure 4 (a) displays snapshot patterns of the spiral wave at the times represented by symbols (a)~(f) in Fig. 3 (a). At $t = 11$ the spiral wave without control stably-rotates. The first impulse with amplitude $u^* = 330$ is injected at $t = 12$. After that, the most of the excited cells are eliminated, but a few excited cells still remain (see snapshot (b)). The second impulse at $t = 24$ cannot eliminate the remaining excited cells as shown in snapshot (c). Although the impulse injection is repeated, the remaining waves gradually grow. As a result, for $u^* = 330$, the spiral wave cannot be eliminated by the periodic impulse injections.

Figure 4 (b) displays snapshot patterns corresponding to Fig. 3 (b). From snapshots (a) and (b), it can be seen that the wave width becomes slightly narrower by the first impulse at $t = 15$. Control law (3) judges that E_t begins to increase at $t = 20$, and then injects the second impulse into the medium. The wave width is gradually narrowed by repeating injections (see snapshot (c)); consequently, E_t almost monotonically decreases as time proceeds. After the 6th injection, all



(a) Non-feedback control



(b) Feedback control

Figure 4: Snapshot patterns of the spiral wave. The black (white) region represents the excited (rested) cells.

the cells converge on the resting state (see snapshots (d)~(f)). The spiral wave is eventually eliminated by control law (3) with the low-amplitude pulse train.

5. Discussion

Numerical simulations in the preceding section indicate the fact that the timing of signal injections is the most crucial factor to eliminate spiral waves. In particular, we may conclude that the adaptive injection-interval of input signals based on the feedback mechanism is more effective than the periodic injection-interval. However, we still have a problem how to design the amplitude such that spiral waves are eliminated within a given extinction time. In order to solve this problem, it is necessary to reveal the relation among the curvature of waves, the amplitude u^* , and the extinction time τ .

6. Conclusion

This paper compares the performance of the non-feedback control with that of the feedback control for eliminating spiral waves in the CA model. It is clarified on numerical simulations that the feedback con-

troller effectively eliminates spiral waves by the low-amplitude input signals.

References

- [1] S. Sinha and S. Sridhar, in *Handbook of Chaos Control (2nd edition)*, Wiley-VCH Verlag, Weinheim, 2007.
- [2] D. Lindley, Physics for ER, *Physical Review Focus*, 14: story 7, 2004.
- [3] A. V. Panfilov *et al.*, *Phys. Rev. E*, vol. 61, pp. 4644–4647, 2000.
- [4] G.Y. Yuan, S.G. Chen, and S.P. Yang, *Eur. Phys. J. B*, vol. 58, pp. 331–336, 2007.
- [5] G.V. Osipov and J.J. Collins, *Phys. Rev. E*, vol. 60, pp. 54–57, 1999.
- [6] S. Alonso, F. Sagues, and A. S. Mikhailov, *Science*, vol. 299, pp. 1722–1725, 2003.
- [7] S. Alonso, F. Sagues, and A. S. Mikhailov, *Chaos*, vol. 16, pp. 023124, 2006.
- [8] S. Takagi *et al.*, *Phys. Rev. Lett.*, vol. 93, pp. 058101, 2004.
- [9] N.J. Wu *et al.*, *Phys. Rev. E*, vol. 73, pp. 060901, 2006.
- [10] H. Sakaguchi and T. Fujimoto, *Phys. Rev. E*, vol. 67, pp. 067202, 2003.
- [11] H. Sakaguchi and Y. Kido, *Prog. of Theoretical Physics Supplement*, vol. 161, pp. 332–335, 2006.
- [12] A. T. Stamp, G. V. Osipov, and J. J. Collins, *Chaos*, vol. 12, pp. 931–940, 2002.
- [13] S. A. Vysotsky, R. V. Cheremin, and A. Loskutov, *Journal of Physics: Conference Series*, vol. 23, pp. 202–209, 2005.
- [14] H. Sakaguchi and Y. Kido, *Phys. Rev. E*, vol. 71 pp. 1–4, 2005.
- [15] Z. Cao *et al.*, *Europhys. Lett.*, vol. 75, pp. 875–881, 2006.
- [16] H. Zhang, B. Hu, and G. Hu, *Phys. Rev. E*, vol. 68, pp. 026134, 2003.
- [17] Y. Fu *et al.*, *Phys. Rev. E*, vol. 72, pp. 1–5, 2005.
- [18] G. Yuan, G. Wang, and S. Chen, *Europhys. Letters*, vol. 72, pp. 908–914, 2005.
- [19] H. Zhang *et al.*, *Phys. Rev. Lett.*, vol. 94, pp. 188301, 2005.
- [20] A. Y. Loskutov and S. A. Vysotskii, *JETP Letters*, vol. 84, pp. 524–529, 2007.
- [21] S. Sinha, A. Pande, and R. Pandit, *Phys. Rev. Lett.*, vol. 86, pp. 3678–3681, 2001.
- [22] S. Sridhar and S. Sinha, *Europhys. Lett.*, vol. 81, pp. 50002, 2008.
- [23] M. Gerhardt, H. Schuster, and J.J. Tyson, *Physica D*, vol. 46, pp. 392–415, 1990.